

Spatiotemporal light exposure modeling for environmental circadian misalignment and solar jetlag

Trang VoPham^{1a,b,*}, Mimi Ton^{1b,c}, Matthew D. Weaver^{1d,e}

Background: Light exposure is the most powerful resetting signal for circadian rhythms. The objective of this study was to develop and validate a high-resolution geospatial light exposure model that measures environmental circadian misalignment (or solar jetlag) as the mismatch between the social clock and sun clock, which occurs from geographic variation in light exposure leading to delayed circadian phase from relatively less morning light exposure and greater evening light exposure with increasing westward position within a time zone.

Methods: The light exposure model (30 m² spatial resolution) incorporated geospatial data across the United States on time zones, elevation (using Google Earth Engine), sunrise time, and sunset time to estimate solar jetlag scores (higher values indicate higher environmental circadian misalignment). The validation study compared the light exposure model in 2022, which was linked with geocoded residential addresses of n = 20 participants in Boston, MA (eastern time zone position) and Seattle, WA (western time zone position) using a geographic information system, with illuminance values captured from wearable LYS light sensors and with sun times from the Solar Calculator.

Results: Western versus eastern positions within a time zone were associated with higher solar jetlag scores from the light exposure model ($P < 0.01$) and relatively larger differences in sunset time measured using light sensors (social clock) and the Solar Calculator (sun clock) ($P = 0.04$).

Conclusion: We developed and validated a geospatial light exposure model, enabling high spatiotemporal resolution and comprehensive characterization of geographic variation in light exposure potentially impacting circadian phase in epidemiologic studies.

Keywords: Light exposure; Circadian disruption; Circadian misalignment; Solar jetlag; Geospatial science

¹Epidemiology Program, Public Health Sciences Division, Fred Hutchinson Cancer Center, Seattle, Washington; ²Department of Epidemiology, University of Washington, Seattle, Washington; ³Cancer Prevention Program, Public Health Sciences Division, Fred Hutchinson Cancer Center, Seattle, Washington; ⁴Division of Sleep and Circadian Disorders, Departments of Medicine and Neurology, Brigham and Women's Hospital, Boston, Massachusetts; and ⁵Division of Sleep Medicine, Harvard Medical School, Boston, Massachusetts

This study was funded by the University of Washington Interdisciplinary Center for Exposures, Diseases, Genomics and Environment (EDGE) Pilot Research Program, which is supported by the National Institutes of Health (NIH)/National Institute of Environmental Health Sciences (NIEHS) P30 ES007033, and the Fred Hutchinson Cancer Center Public Health Sciences Division Bid & Proposal Pilot Program. T.V. was supported by NIH/National Institute of Diabetes and Digestive and Kidney Diseases (NIDDK) K01 DK125612.

A 30 m² spatial resolution geospatial light exposure model can be developed for a specific research study and study population, implementing unique specifications for spatial extent, temporal resolution, and temporal extent. Please visit www.fredhutch.org/lightmodel for information on how to request model development and data access.

SDC Supplemental digital content is available through direct URL citations in the HTML and PDF versions of this article (www.environepidem.com).

*Corresponding Author. Address: Epidemiology Program, Public Health Sciences Division, Fred Hutchinson Cancer Center, 1100 Fairview Ave N, Seattle, WA 98109. E-mail: trang@fredhutch.org (T. VoPham).

Copyright © 2024 The Authors. Published by Wolters Kluwer Health, Inc. on behalf of The Environmental Epidemiology. All rights reserved. This is an open-access article distributed under the terms of the Creative Commons Attribution-Non Commercial-No Derivatives License 4.0 (CCBY-NC-ND), where it is permissible to download and share the work provided it is properly cited. The work cannot be changed in any way or used commercially without permission from the journal.

Environmental Epidemiology (2024) 8:e301

Received 2 November, 2023; Accepted 12 February, 2024

Published online 7 March 2024

DOI: 10.1097/EE9.000000000000301

Introduction

Light is the most powerful synchronizing cue (or zeitgeber) for the circadian system.^{1,2} In mammals, the endogenous circadian system (i.e., biological clock) is comprised of a master circadian pacemaker located in the suprachiasmatic nucleus (SCN) of the hypothalamus.³ The SCN aligns the rhythms of clocks in central and peripheral tissues to maintain a synchronized period of approximately 24 hours.³ Exposure to light (perceived through the eyes) entrains the SCN to the external 24-hour light/dark cycle (i.e., sun clock), which promotes the internal synchronization of biological rhythms and thus optimal functioning for sleep quality, mood, cognitive performance, and metabolism.⁴

Circadian disruption is a disturbance of the biological clock that can occur at and/or between different systemic, organismal, and cellular levels.⁵ Causes of circadian disruption can be internal or external, such as misalignment between the endogenous circadian system with the environmental light/dark cycle

What this study adds:

Light exposure is ubiquitous and is the most powerful resetting signal for circadian rhythms. Circadian misalignment impacts 50% of the population. We developed and validated a novel high-resolution geospatial light exposure model to measure environmental circadian misalignment or solar jetlag (resulting from geographic variation in light exposure due to location within a time zone), incorporating data on time zones, elevation, sunrise time, and sunset time. This geospatial methodology is scalable, allowing for the development of a 30 m² spatial resolution light exposure model that can be linked with any study population around the world for any time period to conduct epidemiologic research.

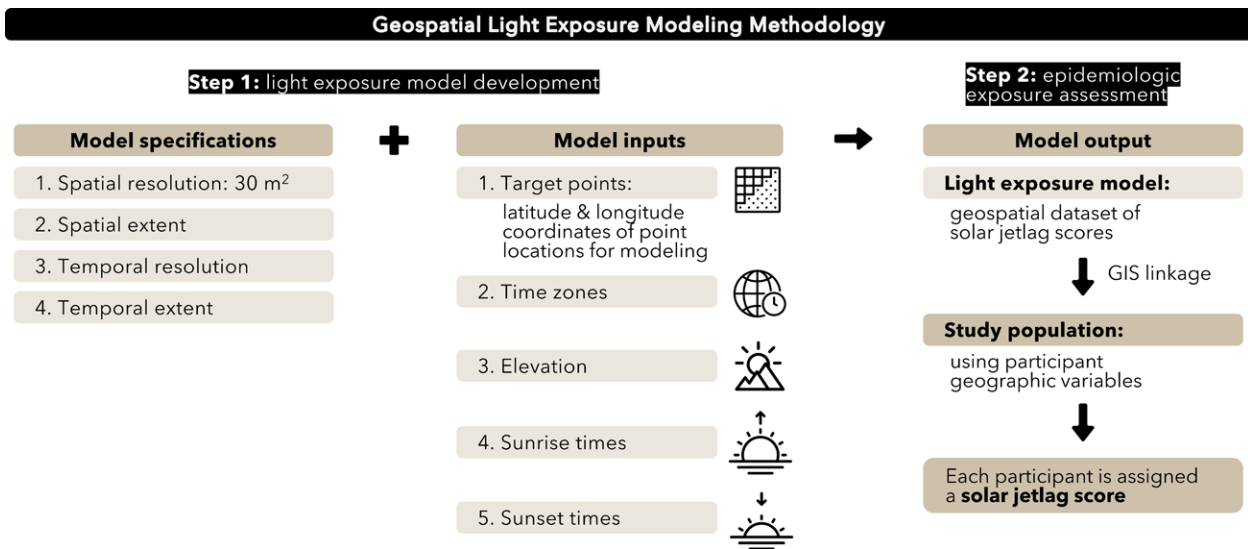


Figure 1. Geospatial light exposure modeling methodology. Step 1 of the geospatial workflow to create a light exposure model to estimate environmental circadian misalignment or solar jetlag (i.e., mismatch between the social clock and sun clock) is comprised of defining model specifications of the spatial resolution (fixed at a granular 30 m²), spatial extent, temporal resolution, and temporal extent. The model inputs include target points, time zones, elevation, sunrise times, and sunset times, which are utilized to create the light exposure model that is linked with participant geographic variables in a study population using GIS (Step 2, epidemiologic exposure assessment). Each participant is assigned a solar jetlag score, with higher values indicating higher environmental circadian misalignment.

or the behavioral feeding/fasting cycle.^{5,6} Circadian misalignment describes a specific type of circadian disruption that can occur at different biological levels relative to the systemic level and is comprised of an abnormal phase angle between two or more rhythms that may be internal and/or external.^{5,7}

In circadian biology, the biological clock refers to the endogenous circadian system, the social clock refers to our social and work commitments, and the sun clock refers to the light/dark cycle.^{8–10} Circadian disruption occurs when there is a misalignment between the biological clock and the sun clock.^{7,11} Sources of circadian disruption, which include night shift work and social jetlag, have been associated with adverse human health outcomes including cancer.⁴ Another source of circadian disruption is the timing of environmental light exposure due to geographic location within a time zone, which we hereafter refer to as environmental circadian misalignment or solar jetlag and is defined as the mismatch between the social clock and the sun clock.^{12,13} In particular, individuals located within a time zone tend to adhere to a common social time (e.g., work day begins at 9 am local time). However, since the sun rises in the east and progresses to set in the west, individuals who are located in the western region of a time zone are subject to relatively less light exposure early in the morning and greater light exposure later in the day compared with individuals located in the eastern region of the same time zone.^{2,14} This geographic variability in the timing of environmental light exposure (and thus differential exposure to light based on location within a time zone) may increase the likelihood of a later phase of entrainment to the 24-hour day among individuals located in the western region of a time zone, who may experience light exposure later in the evening, but are still expected to awaken at the same local clock time for work, school, and social commitments.

Previous epidemiologic studies have conducted exposure assessments measuring environmental circadian misalignment using participant residential locations combined with geographic locations within a time zone only.^{12,15} To date, there is no exposure measure that incorporates other important predictors of environmental circadian misalignment (beyond location within a time zone) that would enable comprehensive characterization of geographic variation in environmental light exposure contributing to misalignment of circadian rhythms.

The objective of this study was to develop and validate a high-resolution geospatial light exposure model to assess environmental circadian misalignment or solar jetlag, or the mismatch between the social clock and the sun clock. This geospatial light exposure modeling methodology combines granular data on location within a time zone, elevation, sunrise time, and sunset time, and can be scaled to model any study area around the world and for any time period of interest. A secondary objective of this study was to validate the geospatial light exposure model using wearable light sensors.

Methods

Figure 1 shows the geospatial light exposure modeling methodology workflow to estimate a solar jetlag score for a study participant in an epidemiologic study, incorporating granular geospatial datasets on time zones, elevation (using Google Earth Engine),¹⁶ sunrise times, and sunset times. Higher values for the solar jetlag score indicate higher environmental circadian misalignment as the mismatch between the social clock and the sun clock. This geospatial modeling methodology is scalable, with a workflow enabling flexibility in the estimation of the solar jetlag score (at a 30 m² spatial resolution) to conduct epidemiologic research for any geographic variable available in a study population, study area across the world, temporal resolution, and/or any time period of interest.¹⁷

Modeling methodology step 1: light exposure model development

To develop a light exposure model, the following model specifications are defined: (1) The spatial resolution of the light exposure model is fixed at a highly granular 30 m² level, where solar jetlag scores are estimated at point locations (specified by latitude and longitude coordinates) that are positioned 30 m apart—hereafter referred to as target points. (2) The spatial extent is specified as the study area of the light exposure model and can extend to any geographic area across the world. (3) The temporal resolution of the light exposure model is determined by the target frequency of estimates. For example, potential

temporal resolutions include daily (i.e., highest temporal resolution), weekly, monthly, seasonal, and yearly. The temporal resolution guides the calculations for the sunrise times and sunset times as part of the solar jetlag score. Relatedly, the temporal resolution of the light exposure model can be applied to any given (4) temporal extent or time span or period of interest.

The following model inputs are required to develop a light exposure model: Using a geographic information system (GIS), the (1) target points (30 m) are spatially joined with (2) time zone boundaries to determine each target points' relative location within a time zone. (3) Elevation (in units of meters) is determined through spatially joining the target points with a digital elevation model (DEM) raster developed closest in time to the temporal extent. Local topography influences sun exposure, with higher elevation generally removing obstructions and extending the field of view, resulting in an earlier sunrise and a later sunset, and thus greater environmental circadian misalignment.¹⁸ Although an earlier sunrise would result in a phase advance, a later sunset would additionally result in a phase delay.^{19,20} Using equations from Astronomical Algorithms by Meeus,^{21,22} (4) sunrise time (in units of hours, minutes, and seconds) is calculated at the target point and at the point location at the eastern-most boundary of the time zone in which the target point is located (holding latitude constant). The eastern-most boundary of the time zone is used as the reference because it is associated with the least amount of environmental circadian misalignment as intrinsic circadian rhythms are slightly longer than 24 hours on average and require a slight advance each day to maintain alignment, which is promoted by more light exposure in the morning hours and less light exposure in the evening hours.²³ The difference between the sunrise time at the target point and the eastern-most time zone boundary point location is averaged over the temporal resolution for a given temporal extent. Similar to sunrise time, astronomical equations^{21,22} are used to calculate (5) sunset time (in units of hours, minutes, and seconds) at the target point and at the point location at the eastern-most boundary of the time zone in which the target point is located (holding latitude constant). The difference between the sunset time at the target point and the eastern-most time zone boundary point location is averaged over the temporal resolution for a given temporal extent. As the Earth's tilt results in differential light exposure based on latitude, the light exposure model workflow incorporates latitude through the sunrise time and sunset time calculations that estimate time differences between the two locations (target point and corresponding point at eastern-most time zone boundary) at the same latitude.²⁴ Higher differences in sunrise time (or sunset time) between the target point and eastern-most time zone boundary point location indicate higher environmental circadian misalignment or a greater mismatch between the social clock and the sun clock.

Modeling methodology step 2: epidemiologic exposure assessment

Using these aforementioned model inputs of target points, time zone boundaries, elevation, sunrise time, and sunset time, the model output is the light exposure model comprised of a geospatial dataset of solar jetlag scores estimated at each target point that has been specifically developed at a 30 m² spatial resolution for the specified spatial extent, temporal resolution, and temporal extent. At each target point, a solar jetlag score is calculated by summing the weighted quantile ranks for elevation, sunrise time, and sunset time, where the calculation weights sunrise time (0.45) and sunset time (0.45) more compared with elevation (0.10) because changes in elevation result in relatively smaller differences in light exposure compared with sunrise time and sunset time (see equation).^{25,26} Quantile rankings are determined based on the distribution of each of these variables separately within each time zone, which accounts for

how local time is determined based on a given time zone and for differences in east to west extent of time zones. Values for sunrise time and sunset time represent the difference between the sun time at the target point and the eastern-most time zone boundary point location.

$$\begin{aligned} \text{solar jetlag score}_{\text{target point}} &= \{(\text{elevation}_{\text{quantile rank within time zone}}) \times 0.10\} \\ &+ \{(\text{sunrise time difference}_{\text{quantile rank within time zone}}) \times 0.45\} \\ &+ \{(\text{sunset time difference}_{\text{quantile rank within time zone}}) \times 0.45\} \end{aligned}$$

Thus, target points located in different time zones that are characterized by a similar mismatch between the social clock and sun clock based on a similar distance between the target point and the location at the eastern-most time zone boundary (holding latitude constant) may not receive a similar solar jetlag score because of the stratified approach to account for time zone.

To conduct an exposure assessment for light exposure in an epidemiologic study, using GIS, study participant geographic variables are spatially joined with the light exposure model. Any geographic variable available in a study population can be linked with the light exposure model such as geocoded residential addresses (i.e., street addresses assigned latitude and longitude coordinates) and administrative units (e.g., census blocks, census block groups, census tracts, and zip codes). To determine the solar jetlag score for each study participant, the GIS linkage is conducted as a spatial overlay between the light exposure model and study participant geographic variables. Any geographic variables that are polygons, such as census tracts, are assigned appropriate point locations (e.g., center of population, centroid) to execute the scientifically optimal geospatial analyses.

Application of geospatial light exposure modeling methodology

To demonstrate the application of the geospatial light exposure modeling methodology in practice, we developed a light exposure model (30 m² spatial resolution) for the spatial extent of the United States (including Washington, DC and Puerto Rico), at a yearly average temporal resolution and in the temporal extent of 2022. Target points were created using a geospatial fishnet procedure to produce regular 30 m² grids across the spatial extent. Target points were spatially joined with time zone boundaries maintained by Esri²⁷ to determine to which time zone they belonged. To determine elevation, target points were spatially joined with NASADEM elevation data using Google Earth Engine, a cloud computing platform enabling storage and processing of spatial big data for geospatial analyses using Google's cloud resources.^{16,28–30} NASADEM is a high-resolution (30 m²) global DEM raster dataset that has been ingested into (i.e., archived) Google Earth Engine for open-source use.³¹ NASADEM data products were developed through a reprocessing of satellite remote sensing Earth observation (EO) images from the Shuttle Radar Topography Mission (SRTM; collecting data in 2000) and combining auxiliary data from Terra Advanced Spaceborne Thermal and Reflection Radiometer (ASTER), Ice, Cloud, and Land Elevation Satellite (ICESat) Geoscience Laser Altimeter System (GLAS) Lidar, and Advanced Land Observing Satellite Panchromatic Remote-sensing instrument for Stereo Mapping (PRISM).^{32–34} The geemap Python package, using the Jupyter Notebook environment, was utilized to export target points spatially joined with elevation data from Google Earth Engine for local geospatial analyses.^{35,36} Since there was missing geographic coverage in NASADEM for Alaska, target points located in Alaska were spatially joined with the United States Geological Survey 3D Elevation Program DEM (5 m² spatial resolution).³⁷ Separately for sunrise time and sunset time, the

yearly average difference (in minutes) was calculated between the sunrise time (or sunset time) at the target point location and the sunrise time (or sunset time) at the point location at eastern-most time zone boundary (holding latitude constant; averaged across each day in 2022 to calculate the yearly average).^{21,22} For each target point, a solar jetlag score was calculated by summing percentile ranks (0–99) for elevation, sunrise time (difference), and sunset time (difference), where percentile ranks were determined separately by time zone and the following weights were applied in the summation for elevation (0.10), sunrise (0.45), and sunset (0.45). Geospatial analyses utilized the WGS84 geographic coordinate system (default for Google Earth Engine) and created maps utilized one of the following projected coordinate systems: contiguous US Albers equal-area conic (NAD83 datum; USGS version) or Alaska Albers (NAD83 datum; 2011 version). All geospatial analyses were conducted using Google Earth Engine, geemap, and ArcGIS Pro version 3.1 (Esri, Redlands, CA).

Daylight saving time

For some countries, such as the United States, Daylight Saving Time (DST) occurs between the spring and fall every year.³⁸ Standard Time is the period outside of DST. The two US states of Arizona and Indiana do not observe DST.³⁹ The DST transition is initiated in the spring by turning clocks forward 1 hour, which results in the social clock becoming later than the sun clock as there is a greater amount of light exposure in the evening.^{10,38} To account for DST in the light exposure modeling workflow, separate light models could be created to produce solar jetlag scores at a daily temporal resolution during a time period before the DST transition, an acute period following the DST transition (e.g., Monday through Friday following DST),³⁹ and a time period after schedules have adjusted to DST.

Validation study of the light exposure model using wearable light sensors

We conducted a validation study to compare solar jetlag scores (derived from GIS linkage of participant geocoded residential addresses with the light exposure model) with light intensity measures from wearable light sensors. A total of 20 participants were recruited in 2022, with $n = 10$ participants residing in Boston, MA (on the eastern edge of the Eastern time zone; hereafter referred to as the eastern position in time zone) and $n = 10$ participants residing in Seattle, WA (on the western edge of the Pacific time zone; hereafter referred to as western position in time zone). Participants were healthy adults (aged 18 years or older), owned an iPhone, were not traveling outside of the Seattle, WA (or Boston, MA) metropolitan areas for more than 2 consecutive days during the study period, and did not work night shifts. Participants completed a baseline questionnaire collecting information on sociodemographics, body mass index, time activity patterns, and residential locations, which was administered online using REDCap.

Each participant was asked to wear a LYS Button light sensor on their clothing for 2 weeks. The LYS Button is a wearable sensor that is comprised of a tristimulus filter array that collects ambient visible and near-infrared wavelengths (380–1,100 nm; peak sensitivities at 465, 525, and 615 nm) and photopic illuminance (i.e., perceived visible brightness of a scene) from 0 to 100,000 lux at a 15-second sampling rate.^{40–42} The sensor has a mean standard error of 5%–10% depending on intensity, with an engineered propensity to indoor lighting scenes (i.e., illuminances between 0 and 500 lux). Participants were instructed to place the sensor as close to their eye as possible, such as on their shirt collar, and to charge their sensor each night (with the charging dock placed next to their bed). Each light sensor was linked to the participant's smartphone using the LYS iPhone

app, which enabled Bluetooth syncing of data and transmission to a cloud-based server. Each collected light measurement was accompanied by a date and time stamp. The participants provided written informed consent and the study was approved by the Fred Hutchinson Cancer Center Institutional Review Board.

Statistical analysis

For the validation study, to represent a participant's social clock, we used data collected on the intensity of illuminance values and the associated date and time stamps from the LYS light sensors to calculate sunrise time and sunset times. Illuminance values were averaged into 10-minute intervals.⁴³ We excluded days during which less than 24 hours of illuminance values were collected (data lapses may have occurred if the iPhone hosting the LYS app was not placed within 10 m of the LYS light sensor at least once per day to enable Bluetooth data transfer)⁴⁰ or days with no illuminance values ≥ 100 lux (which may indicate lack of sensor exposure to indoor or outdoor light).⁴⁴ The sunrise time was defined as the first instance on a given day during which the average illuminance values for at least 50 consecutive minutes (corresponding to the average time in bed after wake time)⁴⁵ were ≥ 100 lux⁴⁴ and that did not occur between 5 pm and 1 am.⁴⁵ The sunset time was defined as the first instance occurring after the sunrise time on a given day (identified using the aforementioned definition) during which illuminance values were < 100 lux⁴⁴ for at least 3 consecutive hours (average time spent in sedentary activities before bedtime)⁴⁶ that was within 20 hours of the sunrise time and was not between 7 am and 5 pm.^{45,47} A given day may have had a valid sunrise time and a missing sunset time if there were no illuminance data collected on the subsequent day to enable a determination of a sunset time occurring within 20 hours of the sunrise time. The variables for sunrise time and sunset time created using LYS light sensor-derived illuminance data represent the participant's onset of light exposure and offset/wind-down of light exposure, respectively, for a given day. Thus, sunrise time and sunset time were used as proxies for each participant's social clock. LYS light sensor data were used as a proxy for each participant's photoperiod (i.e., period of daily illumination received by a person) organized by societal commitments.

To represent a participant's sun clock, we used geocoded residential addresses and the National Oceanic and Atmospheric Administration (NOAA) Solar Calculator to calculate a sunrise time and a sunset time. Participant residential addresses ascertained from questionnaires were geocoded to latitude and longitude coordinates at the street level using ArcGIS Pro version 3.1 (Esri, Redlands, CA). Using the NOAA Solar Calculator, sunrise times and sunset times were calculated for the specific date that the participant contributed data using the LYS light sensor and at their geocoded residential address location. To examine the difference between the social clock and sun clock, signed-rank tests (nonparametric paired t test) were used to examine the differences in sunrise times (and separately for sunset times) estimated using the LYS light sensors versus the NOAA Solar Calculator,^{21,22} overall and stratified by time zone.

To estimate a participant's exposure to environmental circadian misalignment, we calculated the difference (i.e., mismatch) between their social clock (using LYS light sensors) and sun clock (using NOAA Solar Calculator and geocoded residential addresses). To estimate a participant's solar jetlag score, we used GIS to link participant geocoded residential addresses with the light exposure model developed for 2022. Kruskal–Wallis tests were used to examine the associations between location within a time zone (Boston, MA; eastern position in time zone versus Seattle, WA; western position in time zone), solar jetlag scores, and differences in sunrise time (and separately for sunset time) estimated using the LYS light sensor (social clock) and NOAA Solar Calculator (sun clock).

All statistical tests were two-sided. A $P < 0.05$ was considered statistically significant. All times are reported in military time (24-hour clock). Statistical analyses were conducted using SAS 9.4 (SAS Institute, Cary, NC).

Results

Application of the geospatial light exposure modeling methodology in 2022

Figure 2 shows a map of solar jetlag scores (categorized according to quintiles across the spatial extent) from the light exposure model developed at a 30 m² spatial resolution for the United States with a yearly average temporal resolution in 2022 (temporal extent). Higher solar jetlag scores are observed towards the western regions of each time zone (Figure S1; <http://links.lww.com/EE/A265> and Figure S2; <http://links.lww.com/EE/A265>).

Validation study

There were 20 participants included in the validation study, with $n = 10$ residing in Boston, MA (eastern position in time zone) and $n = 10$ residing in Seattle, WA (western position in time zone) (Table 1). The locations of these two cities are shown in Figure S1; <http://links.lww.com/EE/A265>. Participants were on average 40.75 years old (± 15.54), with the majority self-reporting female sex (65%), White race (60%), and/or non-Hispanic ethnicity (90%). Most participants had a bachelor's degree or higher (90%), were married or in a domestic partnership (30%), and/or were currently employed (90%; of whom 67% were working remotely). Participants had an average body mass index of 25.24 kg/m² (± 4.88) and reported spending an average of 2.56 hours (± 2.10) outdoors each day and leaving their home 2.70 times (± 1.75) each day. The average solar jetlag score was 44.49 ± 33.35 . Participants residing in Seattle, WA (western position in time zone) were slightly older, spent a higher amount of time outdoors, and/or had higher solar jetlag scores, while a higher proportion of participants in Boston, MA (eastern position in time zone) were currently employed.

The $n = 20$ participants in this study contributed a total of 213 days of data from 19 August 2022 to 20 October 2022 (Table 2). Of these days, 213 days had estimated sunrise times and/or sunset times, of which 206 days had estimated sunrise times and sunset times, and the remaining 7 days had estimated sunrise times but no sunset times because no data were collected on the subsequent day to enable determination of a sunset time within 20 hours of the sunrise time. Participants residing in Boston, MA (eastern position in time zone) contributed 92 sunrise times and 88 sunset times, and participants residing in Seattle, WA (western position in time zone) contributed 121 sunrise times and 118 sunset times. Overall, the median sunrise time estimated using LYS light sensors (social clock) (8:00, inter-quartile range [IQR]: 7:00–8:40) was later compared with using the NOAA Solar Calculator (sun clock) (5:24, IQR: 5:14–5:33) (difference between LYS and Solar Calculator medians: 2 hours 36 minutes) ($P < 0.01$). Similar differences were observed among participants in Boston, MA (eastern position in time zone) ($P < 0.01$) and among participants in Seattle, WA (western position in time zone) ($P < 0.01$).

The median sunset time estimated using LYS light sensors (19:20, IQR: 18:00–20:20) was later compared with using the Solar Calculator (18:35, IQR: 18:14–18:51) (difference between LYS and Solar Calculator medians: 25 minutes) ($P < 0.01$). Similar differences were observed among participants in Seattle, WA (western position in time zone) ($P < 0.01$). Among participants in Boston, MA (eastern position in time zone), the median sunset time was similar when estimated using LYS sensors compared with the NOAA Solar Calculator.

There were associations between the solar jetlag score, time zone location, and differences in sunrise time (or sunset time) measured using the LYS light sensors (social clock) and the Solar Calculator (sun clock) (Table 3). Solar jetlag scores were higher among participants in Seattle, WA (western position in time zone; median 73.70, IQR: 73.40–73.80) compared with participants in Boston, MA (eastern position in time zone; median 6.40, IQR: 6.10–6.40) ($P < 0.01$). The difference in sunrise times estimated using LYS light sensors and the Solar Calculator was larger among participants in Boston, MA (median 3:03, IQR: 1:58–3:38) compared with Seattle, WA (median 2:03, IQR: 1:22–3:00) ($P < 0.01$). In contrast, the difference in sunset times estimated using LYS light sensors and the

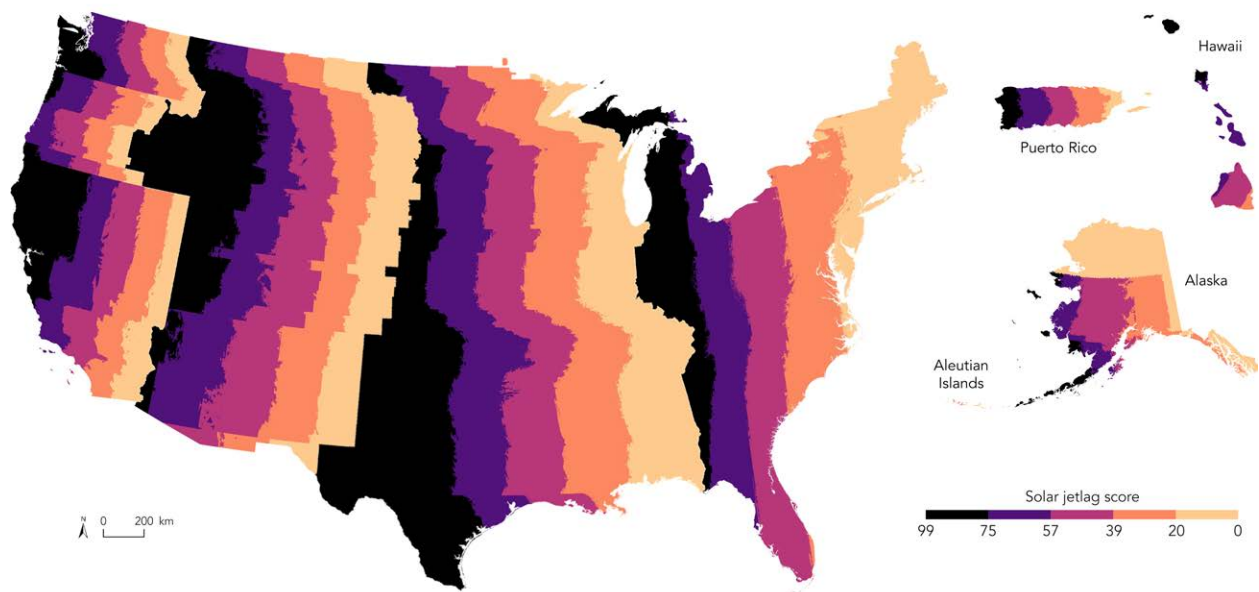


Figure 2. Light exposure model for the United States in 2022. The light exposure model was developed for the United States, including Washington, DC and Puerto Rico. The spatial resolution is 30 m² with a yearly average temporal resolution in 2022. The map is categorized by quintiles of the solar jetlag score estimated across all time zones.

Table 1.**Population characteristics of participants in the validation study using LYS light sensors from August to October 2022**

| Variable | Overall (n = 20) | Boston, MA: eastern position in time zone (n = 10) | Seattle, WA: western position in time zone (n = 10) |
|--|------------------|--|---|
| Age (years); (mean ± SD) | 40.75 ± 15.54 | 37.80 ± 14.67 | 43.70 ± 16.60 |
| Sex (n [%]) | | | |
| Female | 13 (65%) | 7 (70%) | 6 (60%) |
| Male | 7 (35%) | 3 (30%) | 4 (40%) |
| Race (n [%]) | | | |
| White | 12 (60%) | 5 (50%) | 7 (70%) |
| American Indian or Alaska Native, Asian, Black or African American, Native Hawaiian or Pacific Islander, other, or undisclosed | 8 (40%) | 5 (50%) | 3 (30%) |
| Ethnicity (n [%]) | | | |
| Hispanic or Latino | 2 (10%) | 0 (0%) | 2 (20%) |
| Not Hispanic or Latino | 18 (90%) | 10 (100%) | 8 (80%) |
| Bachelor's degree or higher (n [%]) | 18 (90%) | 10 (100%) | 8 (80%) |
| Married or domestic partnership (n [%]) | 6 (30%) | 3 (30%) | 3 (30%) |
| Currently employed (n [%]) | 18 (90%) | 10 (100%) | 8 (80%) |
| Among employed: remote working (n [%]) | 12 (67%) | 7 (70%) | 5 (63%) |
| BMI (kg/m ²); (mean ± SD) | 25.24 ± 4.88 | 23.53 ± 3.28 | 26.95 ± 5.75 |
| Daily hours spent outdoors (mean ± SD) | 2.56 ± 2.10 | 1.85 ± 0.94 | 3.28 ± 2.69 |
| Daily times leaving home (mean ± SD) | 2.70 ± 1.75 | 2.00 ± 0.94 | 3.40 ± 2.12 |
| Solar jetlag score (mean ± SD) | 44.49 ± 33.35 | 6.34 ± 0.34 | 73.50 ± 0.47 |

BMI indicates body mass index; SD, standard deviation.

Table 2.**Comparison of sunrise times and sunset times estimated using LYS light sensors and NOAA Solar Calculator from August to October 2022**

| | Overall (n = 20) | | | | Boston, MA: eastern position in time zone (n = 10) | | | | Seattle, WA: western position in time zone (n = 10) | | | |
|---------------------------|---------------------------|---------------------|------------------------------------|----------------|--|---------------------|------------------------------------|----------------|---|---------------------|------------------------------------|----------------|
| | Social clock ^a | | Sun clock | | Social clock ^a | | Sun clock | | Social clock ^a | | Sun clock | |
| | LYS ^b | | NOAA Solar Calculator ^b | | LYS ^b | | NOAA Solar Calculator ^b | | LYS ^a | | NOAA Solar Calculator ^b | |
| | n | (median [IQR]) | (median [IQR]) | P ^c | n | (median [IQR]) | (median [IQR]) | P ^c | n | (median [IQR]) | (median [IQR]) | P ^d |
| Sunrise time ^c | 213 | 8:00 (7:00–8:40) | 5:24 (5:14–5:33) | <0.01 | 92 | 8:20 (7:25–8:50) | 5:14 (05:08–5:24) | <0.01 | 121 | 7:30 (6:50–8:30) | 5:29 (5:22–5:34) | <0.01 |
| Sunset time ^c | 206 | 19:20 (18:00–20:20) | 18:35 (18:14–18:51) | <0.01 | 88 | 18:00 (18:00–19:50) | 18:11 (17:55–18:21) | <0.01 | 118 | 19:40 (18:50–20:30) | 18:49 (18:41–18:58) | <0.01 |

^aSunrise times and sunset times created using illuminance data from LYS light sensors represent the onset and offset/wind-down of light exposure (respectively) and each participant's photoperiod organized by societal commitments and were used as a proxy for their social clock.

^bAll values are presented in local time.

^cA total of 213 days had estimated sunrise times and/or sunset times and 206 had estimated sunrise times but no sunset times because no data were collected on the subsequent day to enable determination of a sunset time within 20 hours of the sunrise time.

^dSigned-rank tests.

Table 3.**Associations between solar jetlag scores, time zone location, and differences in sun time estimated using LYS light sensors and NOAA Solar Calculator**

| | Boston, MA: eastern position in time zone (n = 10) | | Seattle, WA: western position in time zone (n = 10) | | P ^a |
|---|--|-------------------|---|---------------------|----------------|
| | n | median (IQR) | n | median (IQR) | |
| Solar jetlag score ^b | 92 | 6.40 (6.10–6.40) | 121 | 73.70 (73.40–73.80) | <0.01 |
| Sunrise time difference (social clock—sun clock) ^c | 92 | 3:03 (1:58–3:38) | 121 | 2:03 (1:22–3:00) | <0.01 |
| Sunset time difference (social clock—sun clock) ^c | 88 | 0:31 (–0:09–1:58) | 118 | 0:47 (–0:07–1:28) | 0.04 |

^aKruskal-Wallis tests.

^bSolar jetlag scores are unitless and values range from 0 to 99. Higher values indicate higher environmental circadian misalignment.

^cAll values are expressed as differences in hours and minutes in local time between the social clock (estimated using LYS light sensors) and the sun clock (estimated using the NOAA Solar Calculator).

Solar Calculator was slightly larger among participants in Seattle, WA (median 0:47, IQR: –0:07–1:28) compared with Boston, MA (median 0:31, IQR: –0:09–1:58) ($P = 0.04$). Similar results were

observed when using alternative weighting for elevation, sunrise time, and sunset time (Supplemental Table S1; <http://links.lww.com/EE/A265>).

Discussion

This study presents a novel spatiotemporal light exposure model validated using wearable light sensors, which can be linked with location-based information in study populations to conduct epidemiologic studies on exposure to solar jetlag or environmental circadian misalignment as the mismatch between the social clock and sun clock. This model integrates the latest technologies in geospatial big data and data science, including the Google Earth Engine cloud-based geospatial analysis platform. The geospatial workflow used to develop the light exposure model is characterized by a highly resolved spatial resolution of 30 m² and is scalable in terms of spatial extent, temporal resolution, and temporal extent. Thus, this geospatial light exposure model can be developed for any study area and any time period, enabling flexibility in investigating epidemiologic research questions.

The geospatial light exposure model quantifies the mismatch between the social clock and the sun clock, which is an important aspect of circadian disruption. There are three clocks governing circadian biology: (1) the biological clock in circadian time that controls our physiology (i.e., endogenous circadian system), (2) the social clock in local time that organizes our lives (e.g., work, school, and social commitments), and (3) the sun clock in solar time that is derived from the natural 24-hour light/dark schedule set by the sun.^{8–10} The biological clock requires zeitgebers to entrain (or synchronize) to the sun clock (rather than the social clock), with the strongest zeitgebers being environmental light from the sun.^{1,2,48} The phase of entrainment refers to the alignment of the biological clock with the sun clock,⁴⁹ and chronotype is defined as the variability in phase of entrainment.^{49,50} Chronotypes are likely established by genetics, age, sex, and light exposure.⁴⁸

Circadian disruption occurs when there is a mismatch between the biological clock and the sun clock.^{7,11} Sources of circadian disruption include night shift work and social jetlag.^{51,52} Night shift work is defined as work during the regular sleeping hours of the general population, which perturbs the natural cycle of sleep and wakefulness and related patterns of activity and rest, and thus may disrupt circadian rhythms.⁵¹ The International Agency for Research on Cancer classified night shift work as a Group 2A probable human carcinogen.⁵¹

Social jetlag is defined as the mismatch between the biological clock and the social clock.^{51,52} Social jetlag is estimated as the difference in the midpoint of sleep between the work week and (work-free) weekend days, assuming that individuals live more according to their social clock during the work week versus more according to their biological clock on work-free days.⁴⁸ Social jetlag is driven by early rise times for school and work, in addition to widespread use of artificial indoor lighting and technologies (e.g., smartphones, televisions, and computers) that emit short wavelength blue light, which is effective in suppressing melatonin and thus reduces the propensity to sleep.^{49,52–55} Social jetlag leads to a chronic sleep debt due to earlier and shorter sleep on workdays/weekdays, which is then compensated through later and longer catch-up sleep on work-free days.^{49,54} This chronic circadian misalignment between rapidly shifting, self-selected light-dark exposure and an unchanged solar day-night cycle creates a situation resembling sleep-wake patterns frequently observed in travel that crosses time zones.⁵⁴ A common characteristic of social jetlag is increased exposure to light in the evening, resulting in a phase delay of the biological clock and a shift in the chronotype distribution such that there are more late chronotypes (i.e., social jetlag is more pronounced in late chronotypes).⁵⁴ Social jetlag is highly prevalent in the population, with estimates upwards of 50% of individuals impacted.^{52,56,57} In a study examining the National Health and Nutrition Examination Survey in the United States, among adults aged 20 years or older, 46.5% experienced at least 1 hour of social jetlag.⁵⁷ Social jetlag has also been implicated as a risk factor for a variety of adverse health outcomes including obesity and mental health symptoms.^{48,58}

Solar jetlag, which is objectively measured using solar jetlag scores from our light exposure model, is defined as the mismatch between the social clock and the sun clock and is a source of chronic environmental circadian misalignment. Solar jetlag is a term coined by Reis et al¹³ to refer to the extent to which people are living displaced from the sun clock. Although individuals located within a time zone adhere to a common social time, the amount of light from the sun to which a person is exposed will vary depending on location within a time zone.⁵⁹ Due to the Earth's rotation, the sun progresses in the sky from east to west at a rate of 4 minutes per each degree of longitude, which results in a later sunset moving east to west within a time zone. This differential light exposure that drives solar jetlag is expected to exacerbate the consequences of social jetlag because of modern societal schedules. In particular, increasing solar jetlag due to westward location within a time zone would be compounded by the effects of work and school commitments occurring at early times (i.e., social jetlag), humans spending a large amount of time inside buildings with relatively low light levels compared with daylight in the outdoors, and experiencing a lack of darkness during the night due to the pervasiveness and availability of artificial light,¹³ all of which would culminate in less sleep duration.¹³

In particular, the light exposure model captures environmental circadian misalignment (as the mismatch between the social clock and sun clock) due to geographic variation in the timing of light exposure as part of the ambient (outdoor) environment, which is impacted by location within a time zone, elevation, sunrise time, and sunset time. Higher solar jetlag scores indicate residence in locations in the western region of a time zone that are higher in elevation (resulting in fewer obstructions to extend the field of view) and that are characterized by a later sunrise time and a later sunset time (and thus less light exposure in the morning and greater light exposure in the evening), which is hypothesized to promote evening wakefulness during times when sleep would otherwise occur. In a study examining the American Time Use Survey, there was a progressive delay in mid-sleep time on weekends (used as a proxy for chronotype) moving east to west within the Eastern (1.8 minute delay per degree of longitude), Central (1.2 minute delay), and Mountain (2.4 minute delay) time zones in the United States ($P < 0.01$),⁶⁰ showing increasing social jetlag towards the west of a time zone.⁶⁰ As demonstrated in our study, higher solar jetlag scores, due to the east-west movement of the sun across a time zone and higher elevation, also increase moving westward within a time zone.

Although this study demonstrated the application of the geospatial light exposure modeling methodology in the United States for a yearly average temporal resolution in 2022, the geospatial modeling workflow is scalable and the model can thus be expanded globally and across other time periods because of the worldwide availability of model inputs and cloud-based analytics. For example, Esri, a global leader in geospatial science and mapping, maintains an authoritative and updated geospatial dataset of world time zone boundaries.²⁷ NASADEM is a high-resolution geospatial elevation dataset spanning the globe that is available in the Google Earth Engine Data Catalog, which is comprised of an extensive public data archive of worldwide satellite imagery and geospatial datasets.^{31,61} We also applied established astronomical algorithms to estimate sunrise times and sunset times, which can be calculated for any latitude and longitude location on Earth.²¹ Thus, the global geospatial data availability of all model inputs enables linkage of target points (that can be created for any spatial extent and at which solar jetlag scores are estimated) to develop a high spatiotemporal resolution 30 m² light exposure model for any location around the world and for any time period.

We were able to validate the light exposure model using real-world data collected using LYS wearable light exposures

worn by participants residing in different locations within their respective time zones. First, we empirically showed that solar jetlag scores, derived from linking geocoded residential addresses with the light exposure model using GIS, were higher in Seattle, WA (western position in time zone) compared with Boston, MA (eastern position in time zone). Second, we demonstrated that there was evidence of environmental circadian misalignment, defined as differences in the social clock (estimated using LYS light sensors) and sun clock (estimated using NOAA Solar Calculator). To estimate a participant's social clock, we used illuminance data collected from the LYS light sensors as a proxy because the sensor captures illuminance from all sources including the sun, indoor artificial lighting, and screen technologies and thus the participant's photoperiod organized by societal commitments.^{40–42} To estimate a participant's sun clock, we used the NOAA Solar Calculator to calculate precise sun times at their geocoded residential addresses. We observed differences between the social clock and the sun clock, where the social clock was generally later compared with the sun clock overall and by time zone position.

In the analyses for sunrise time, the social clock was consistently later than the sun clock, with a smaller difference in Seattle, WA (western position in time zone) compared with Boston, MA (eastern position in time zone) and where LYS-based sunrise times were relatively earlier among residents in Seattle, WA. This suggests that participants with higher solar jetlag scores residing in Seattle, WA had wake times closer to the actual sunrise. This finding may be attributable to increased exposure to natural light (with more time spent outdoors and away from home), having wake times closer to sunrise for work commitments, and/or due to earlier wake times with older age.⁶² Further, a higher proportion of participants in Boston, MA were employed and may thus have work, social, and other commitments necessitating hours of indoor wakefulness into the evening and resulting in later wake times, may experience relatively more social jetlag, and/or maybe more likely to be late chronotypes given their relatively younger age. In contrast, in the analyses for sunset times, there was a slightly larger difference in a later social clock versus sun clock in Seattle, WA (western position in time zone) versus Boston, MA (eastern position in time zone), with Seattle participants having a social clock approximately 47 minutes later than the sun clock, and Boston participants having a social clock approximately 31 minutes later than the sun clock.

Altogether, the validation study demonstrated that higher solar jetlag scores were observed in the western compared with the eastern position in a time zone, and that the western position in a time zone was associated with a slightly larger difference in the social clock compared with the sun clock (for the sunset time). Environmental circadian misalignment, or the mismatch between the social clock and the sun clock, is expected to be higher in the western position of a time zone due to less light exposure early in the morning and greater light exposure later in the day. Overall, the validation study demonstrated that the light exposure model may serve as a useful proxy to identify individuals who experience greater environmental circadian misalignment (or a greater mismatch between the social clock and the sun clock) and thus exposed to solar jetlag based on their geographic location within a time zone.

Importantly, the light exposure model provides a high-resolution, validated approach to measuring environmental circadian misalignment, which is a modifiable risk factor for many disease outcomes.^{12,14,15,63} Viable interventions include exposure to light at appropriate times of day, such as bright light in the morning or avoidance of light in the evening, which promotes a phase advance shifting individuals to an earlier biological time and may reduce circadian misalignment for individuals in the western region of a time zone exposed to delayed sunrise and sunset times.⁶⁴ Timed light exposure is an intervention that has been piloted in patients with liver disease and delayed sleep-wake

rhythms to mitigate the consequences of circadian misalignment.⁶⁵ In addition, irrespective of location in a time zone, sleep health can be promoted through behavioral and environmental modifications such as limiting exposure to light at night (e.g., window shades and/or eye masks), optimizing sleep timing, duration, and regularity of sleep, regular exercise, and limiting the use of devices that emit blue-enriched light at night.^{55,63,66,67} At the policy level, implementing schedules designed to facilitate alignment of social or work commitments with biological time, such as delayed school start times, has demonstrated reductions in circadian disruption.^{68,69}

There were some limitations of this study. The light exposure model does not incorporate a measure of internal time (i.e., biological clock). However, the results of the validation study demonstrate the utility of solar jetlag scores as a proxy measure for environmental circadian misalignment (i.e., mismatch between the social clock and sun clock) due to differential light exposure from position in a time zone. We estimated sunrise time and sunset time using illuminance measurements from the LYS light sensor, which may not reflect the actual wake time and bedtime of each participant. However, we utilized established thresholds for illuminance values relevant to chronobiology and data on sleep timing and sedentary behaviors to determine sensor-based sunrise times and sunset times.^{44–47} There may have been measurement error from participants inconsistently wearing the sensor and/or wearing the sensor incorrectly (e.g., clothing covering the sensor). However, trained study personnel provided each participant with detailed information from LYS regarding the appropriate use of the sensor and app. Although the light exposure model provides a solar jetlag score as a measure of environmental circadian misalignment, the model does not include information on time activity patterns such as time spent outdoors, personal behaviors regarding light modification and usual sleep habits, and cloud cover which may impact outdoor light exposure (though the resetting effect of sunlight with cloud cover is robust).⁷⁰ However, the light exposure model is the highest spatial and temporal resolution geospatial exposure model developed to date, incorporating important predictors of geographic variation in environmental light exposure, and can be combined with other individual-level information available in study populations to assess and examine circadian misalignment.

Strengths of this work include the development of a scalable, high spatiotemporal resolution geospatial methodology that is able to create a light exposure model to conduct an exposure assessment for an epidemiologic study in any study area and any time period. We have improved on previous research that assessed environmental circadian misalignment using time zone position only^{12,15} through utilizing the highest resolution data inputs to reduce exposure measurement error, including continuously updated geospatial time zone boundaries, highly resolved global elevation data, and sunrise and sunset times estimated at precise latitude and longitude coordinates (point locations). We were able to validate this light exposure model using objective measurements captured by personal light sensors worn by participants across multiple days who resided in the western or eastern region of their respective time zones.

In conclusion, this study presents a novel high-resolution geospatial light exposure model that incorporates granular geospatial data on location within a time zone, elevation, sunrise time, and sunset time that allows for comprehensive characterization of geographic variation in light exposure potentially impacting circadian phase. This high spatiotemporal resolution geospatial modeling workflow is scalable, allowing for the development of a light exposure model at a high spatial resolution (30 m²), and for any spatial extent, temporal resolution, and temporal extent. Thus, the light exposure model can be linked with any study population (using participant geographic variables such as geocoded residential addresses) to execute an epidemiologic exposure assessment of environmental circadian misalignment

to quantify the mismatch between the social clock and the sun clock. Precisely capturing geographic variation in environmental circadian misalignment has important population-level implications as light exposure is ubiquitous and is the most powerful resetting signal for circadian rhythms.

Conflicts of interest statement

The authors declare that they have no conflicts of interest with regard to the content of this report.

Acknowledgments

We would like to express our deepest gratitude to the participants of The Light Study and to the exceptional members of the Fred Hutchinson Cancer Center Cancer Epidemiology Research Cooperative (CERC), in particular Sarah Taylor, April Reitan, David Grogan, and Nancy Blythe, for their time and contributions to this research.

References

- Munch M, Bromundt V. Light and chronobiology: implications for health and disease. *Dialogues Clin Neurosci*. 2012;14:448–453.
- Roenneberg T, Kumar CJ, Mewton M. The human circadian clock entrains to sun time. *Curr Biol*. 2007;17:R44–R45.
- Mohawk JA, Green CB, Takahashi JS. Central and peripheral circadian clocks in mammals. *Annu Rev Neurosci*. 2012;35:445–462.
- Fishbein AB, Knutson KL, Zee PC. Circadian disruption and human health. *J Clin Invest*. 2021;131:e148286.
- Vetter C. Circadian disruption: what do we actually mean? *Eur J Neurosci*. 2020;51:531–550.
- Qian J, Scheer F. Circadian system and glucose metabolism: implications for physiology and disease. *Trends Endocrinol Metab*. 2016;27:282–293.
- Baron KG, Reid KJ. Circadian misalignment and health. *Int Rev Psychiatry*. 2014;26:139–154.
- Roenneberg T. How can social jetlag affect health? *Nat Rev Endocrinol*. 2023;19:383–384.
- Klerman EB, Rahman SA, St Hilaire MA. What time is it? A tale of three clocks, with implications for personalized medicine. *J Pineal Res*. 2020;68:e12646.
- Roenneberg T, Winnebeck EC, Klerman EB. Daylight saving time and artificial time zones - a battle between biological and social times. *Front Physiol*. 2019;10:944.
- Morris CJ, Purvis TE, Hu K, Scheer FA. Circadian misalignment increases cardiovascular disease risk factors in humans. *Proc Natl Acad Sci U S A*. 2016;113:E1402–E1411.
- VoPham T, Weaver MD, Vetter C, et al. Circadian misalignment and hepatocellular carcinoma incidence in the United States. *Cancer Epidemiol Biomarkers Prev*. 2018;27:719–727.
- Reis C, Pilz LK, Kramer A, Lopes LV, Paiva T, Roenneberg T. The impact of daylight-saving time (DST) on patients with delayed sleep-wake phase disorder (DSWPD). *J Pineal Res*. 2023;74:e12867.
- Borisenkov MF. Latitude of residence and position in time zone are predictors of cancer incidence, cancer mortality, and life expectancy at birth. *Chronobiol Int*. 2011;28:155–162.
- Gu F, Xu S, Devesa SS, et al. Longitude position in a time zone and cancer risk in the United States. *Cancer Epidemiol Biomarkers Prev*. 2017;26:1306–1311.
- Gorelick N, Hancher M, Dixon M, Ilyushchenko S, Thau D, Moore R. Google Earth Engine: planetary-scale geospatial analysis for everyone. *Remote Sens Environ*. 2017;202:18–27.
- Fred Hutchinson Cancer Center. Geospatial Light Exposure Model for Environmental Circadian Misalignment and Solar Jetlag <https://www.fredhutch.org/lightmodel>. Accessed 4 January 2024.
- Lisovski S, Hewson CM, Klaassen RH, et al. Geolocation by light: accuracy and precision affected by environmental factors. *Methods Ecol Evol*. 2012;3:603–612.
- Wright KP Jr, McHill AW, Birks BR, Griffin BR, Rusterholz T, Chinoy ED. Entrainment of the human circadian clock to the natural light-dark cycle. *Curr Biol*. 2013;23:1554–1558.
- Crowley SJ, Eastman CI. Phase advancing human circadian rhythms with morning bright light, afternoon melatonin, and gradually shifted sleep: can we reduce morning bright-light duration? *Sleep Med*. 2015;16:288–297.
- Meeus J. *Astronomical Algorithms*. 1st ed. Willmann-Bell; 1991.
- National Oceanic and Atmospheric Administration. NOAA Solar Calculator. <https://gml.noaa.gov/grad/solcalc/index.html>. Accessed 4 January 2024.
- Czeisler CA, Duffy JF, Shanahan TL, et al. Stability, precision, and near-24-hour period of the human circadian pacemaker. *Science*. 1999;284:2177–2181.
- Leocadio-Miguel MA, Louzada FM, Duarte LL, et al. Latitudinal cline of chronotype. *Sci Rep*. 2017;7:5437.
- Diffey BL. Time and place as modifiers of personal UV Exposure. *Int J Environ Res Public Health*. 2018;15:1112.
- Verhulst TG, Stankov SM. Height-dependent sunrise and sunset: effects and implications of the varying times of occurrence for local ionospheric processes and modelling. *Adv Space Res*. 2017;60:1797–1806.
- Esri. World Time Zones <https://www.arcgis.com/home/item.html?id=312cebfea2624e108e234220b04460b8>. Accessed 4 January 2024.
- Tamiminia H, Salehi B, Mahdianpari M, Quackenbush L, Adeli S, Brisco B. Google Earth Engine for geo-big data applications: a meta-analysis and systematic review. *ISPRS J Photogramm Remote Sens*. 2020;164:152–170.
- Kumar L, Mutanga O. Google Earth Engine applications since inception: usage, trends, and potential. *Remote Sens*. 2018;10:1509.
- Zhao Q, Yu L, Li X, Peng D, Zhang Y, Gong P. Progress and trends in the application of Google Earth and Google Earth Engine. *Remote Sens*. 2021;13:3778.
- Google Earth Engine Data Catalog. NASADEM: NASA NASADEM Digital Elevation 30m. https://developers.google.com/earth-engine/datasets/catalog/NASA_NASADEM_HGT_001. Accessed 4 January 2024.
- Crippen R, Buckley S, Agram P, et al. NASADEM global elevation model: methods and progress. *Int Arch Photogramm Remote Sens Spat Inf Sci*. 2016;XLI-B4:125–128.
- National Aeronautics and Space Administration (NASA). NASADEM: Creating a New NASA Digital Elevation Model and Associated Products. <https://www.earthdata.nasa.gov/esds/competitive-programs/measures/nasadem>. Accessed 4 January 2024.
- U.S. Geological Survey (USGS). NASADEM_HGTv001. https://lpdaac.usgs.gov/products/nasadem_hgtv001. Accessed 4 January 2024.
- Wu Q, Lane CR, Li X, et al. Integrating LiDAR data and multi-temporal aerial imagery to map wetland inundation dynamics using Google Earth Engine. *Remote Sens Environ*. 2019;228:1–13.
- Wu Q. geemap: a Python package for interactive mapping with Google Earth Engine. *Journal of Open Source Software*. 2020;5:2305.
- U.S. Geological Survey (USGS). 5 Meter Alaska Digital Elevation Models (DEMs) - USGS National Map 3DEP Downloadable Data Collection. <https://www.sciencebase.gov/catalog/item/5641fe98e4b0831b7d62e758>. Accessed 4 January 2024.
- Roenneberg T, Wirz-Justice A, Skene DJ, et al. Why should we abolish daylight saving time? *J Biol Rhythms*. 2019;34:227–230.
- Fritz J, VoPham T, Wright KP Jr, Vetter C. A chronobiological evaluation of the acute effects of daylight saving time on traffic accident risk. *Curr Biol*. 2020;30:729–735.e2.
- LYS. LYS for research. <https://lystechnologies.io/for-research>. Accessed 4 January 2024.
- Hartmeyer S, Webler F, Andersen M. Towards a framework for light-dosimetry studies: methodological considerations. *Light Res Technol*. 2023;55:377–399.
- Commission Internationale de l'Éclairage. *CIE System for Metrology of Optical Radiation for ipRGC-Influenced Responses to Light: International Standard CIE S 026/E:2018*. CIE; 2018. doi: 10.25039/S026.2018.
- Gwynne SM, Hunt AL, Thomas JR, Thompson AJ, Séguin L. The toilet paper: bathroom dwell time observations at an airport. *Journal of Building Engineering*. 2019;24:100751.
- Gronfier C, Wright KP Jr, Kronauer RE, Czeisler CA. Entrainment of the human circadian pacemaker to longer-than-24-h days. *Proc Natl Acad Sci U S A*. 2007;104:9081–9086.
- Kocevska D, Lysen TS, Dotinga A, et al. Sleep characteristics across the lifespan in 1.1 million people from the Netherlands, United Kingdom and United States: a systematic review and meta-analysis. *Nat Hum Behav*. 2021;5:113–122.
- Matthews CE, Carlson SA, Saint-Maurice PF, et al. Sedentary Behavior in U.S. Adults: Fall 2019. *Med Sci Sports Exerc*. 2021;53:2512–2519.
- Urbanek JK, Spira AP, Di J, Leroux A, Crainiceanu C, Zipunnikov V. Epidemiology of objectively measured bedtime and chronotype

- in US adolescents and adults: NHANES 2003-2006. *Chronobiol Int*. 2018;35:416–434.
48. Roenneberg T, Pitz LK, Zerbin G, Winnebeck EC. Chronotype and social jetlag: a (self-) critical review. *Biology (Basel)*. 2019;8:54.
 49. Taillard J, Sagaspe P, Philip P, Bioulac S. Sleep timing, chronotype and social jetlag: Impact on cognitive abilities and psychiatric disorders. *Biochem Pharmacol*. 2021;191:114438.
 50. Roenneberg T, Wirz-Justice A, Mewes M. Life between clocks: daily temporal patterns of human chronotypes. *J Biol Rhythms*. 2003;18:80–90.
 51. International Agency for Research on Cancer. Night shift work: IARC monographs on the identification of carcinogenic hazards to humans. *World Health Organ*. 2019;124:1–371.
 52. Wittmann M, Dinich J, Mewes M, Roenneberg T. Social jetlag: misalignment of biological and social time. *Chronobiol Int*. 2006;23:497–509.
 53. Wahl S, Engelhardt M, Schaupp P, Lappe C, Ivanov IV. The inner clock-Blue light sets the human rhythm. *J Biophotonics*. 2019;12:e201900102.
 54. Fischer D, Hilditch CJ. Light in ecological settings: entrainment, circadian disruption, and interventions. *Prog Brain Res*. 2022;273:303–330.
 55. Chang AM, Aeschbach D, Duffy JF, Czeisler CA. Evening use of light-emitting eReaders negatively affects sleep, circadian timing, and next-morning alertness. *Proc Natl Acad Sci U S A*. 2015;112:1232–1237.
 56. Koopman ADM, Rauh SP, van 't Riet E, et al. The Association between Social Jetlag, the metabolic syndrome, and type 2 diabetes mellitus in the general population: the New Hoorn Study. *J Biol Rhythms*. 2019;32:359–368.
 57. Di H, Guo Y, Daghlas I, et al. Evaluation of sleep habits and disturbances among US Adults, 2017-2020. *JAMA Netw Open*. 2022;5:e2240788.
 58. Chaput JP, McHill AW, Cox RC, et al. The role of insufficient sleep and circadian misalignment in obesity. *Nat Rev Endocrinol*. 2023;19:82–97.
 59. Giuntella O, Mazzonna F. Sunset time and the economic effects of social jetlag: evidence from US time zone borders. *J Health Econ*. 2019;65:210–226.
 60. Fischer D, Lombardi DA. Chronotypes in the US: influence of longitude position in a time zone. *Chronobiol Int*. 2022;39:460–464.
 61. Google. Earth Engine. <https://earthengine.google.com> Accessed 4 January 2024.
 62. Czeisler CA, Dumont M, Duffy JF, et al. Association of sleep-wake habits in older people with changes in output of circadian pacemaker. *Lancet*. 1992;340:933–936.
 63. Sletten TL, Weaver MD, Foster RG, et al. The importance of sleep regularity: a consensus statement of the National Sleep Foundation sleep timing and variability panel. *Sleep Health*. 2023;9:801–820.
 64. Khalsa SB, Jewett ME, Cajochen C, Czeisler CA. A phase response curve to single bright light pulses in human subjects. *J Physiol*. 2003;549:945–952.
 65. Turco M, Cazzagon N, Franceschet I, et al. Morning bright light treatment for sleep-wake disturbances in primary biliary cholangitis: a Pilot Study. *Front Physiol*. 2018;9:1530.
 66. Murawski B, Wade L, Plotnikoff RC, Lubans DR, Duncan MJ. A systematic review and meta-analysis of cognitive and behavioral interventions to improve sleep health in adults without sleep disorders. *Sleep Med Rev*. 2018;40:160–169.
 67. Brown TM, Brainard GC, Cajochen C, et al. Recommendations for daytime, evening, and nighttime indoor light exposure to best support physiology, sleep, and wakefulness in healthy adults. *PLoS Biol*. 2022;20:e3001571.
 68. Rice A, Sather O, Wright KP, Vetter C, Martin MA, de la Iglesia HO. COVID-19 stay-at-home restrictions increase the alignment in sleep and light exposure between school days and weekends in university students. *Sleep*. 2023;46:zsad059.
 69. Carvalho-Mendes RP, Dunster GP, de la Iglesia HO, Menna-Barreto L. Afternoon school start times are associated with a lack of both social jetlag and sleep deprivation in adolescents. *J Biol Rhythms*. 2020;35:377–390.
 70. Woelders T, Wams EJ, Gordijn MCM, Beersma DGM, Hut RA. Integration of color and intensity increases time signal stability for the human circadian system when sunlight is obscured by clouds. *Sci Rep*. 2018;8:15214.